

# Time-Accurate Aeroelastic Computations of a Full Helicopter Model using the Navier-Stokes Equations

**Guru P. Guruswamy\***

NASA Advanced Supercomputing Division,  
Ames Research Center Moffett Field, CA

## ABSTRACT

A time-accurate procedure to model fluid/structure interactions of helicopter blades is presented. The Navier-Stokes equations in conjunction with the one-equation Spalart-Allmaras turbulence model are used to compute the flow. Structural dynamics is modeled using the modal equations. The aerodynamic and structural dynamic equations are coupled time-accurately using the linear acceleration method of Newmark (direct integration scheme). Effects of time accuracy on the computed results are investigated. Results are compared with experimental data for a full rotor blade system.

**Keywords:** Rotorcraft, Aeroelasticity, Time Integration, CFD

## NOMENCLATURE

[A]	diagonal area matrix of the aerodynamic control points
{Cn, Cm}	sectional lift and moment coefficients
{d}	displacement vector
{F}	generalized aerodynamics force vector
[G]	damping Matrix
Hz	cycles per second
[K]	stiffness matrix
{L}	vector of integrated sectional lift, moment and chord wise aerodynamic forces
[M]	mass matrix
{q}	generalized modal displacement vector
U	the local speed of the blade section
[ $\psi$ ]	the modal matrix

## 1. INTRODUCTION

Aeroelasticity is one of the most challenging fields for both fixed wings and rotating blades [1]. Aeroelastic instabilities “that make or break a vehicle” are caused by strong coupling of fluid and structural forces. Rotary blade systems are inherently flexible and dynamic, requiring time-accurate methods to compute aeroelastic characteristics.

Accurate modeling of helicopter fluid/structure interactions requires the use of high-fidelity fluid and structural models. Computing flows that are dominated by shock wave-boundary layer and blade-vortex interactions requires the use of the 3-D Navier- Stokes equations [2]. The first transonic aeroelastic computation for fixed wings obtained by time accurately coupling the Euler equations with the modal structural equations was presented in Ref. 3. The work in Ref. 3 was based on the success of the original method of time accurately coupling the two dimensional unsteady potential flow equations with the structural equations, as reported in Ref. 4.

The current practice in aeroelastic computations for rotorcraft involves using precomputed displacements from rotorcraft comprehensive methods [5] to solve the Reynolds Averaged Navier-Stokes (RANS) equations and subsequently correcting these displacements using loads obtained from

---

\* Sr. Scientist, Fundamental Modeling and Simulation Branch

the RANS equations. This is an iterative process, which after the requisite number of iterations, yields a periodic solution. Comprehensive methods use measured parameters (such as thrust and moment forces) to compute the control angles [6] instead of using those measured in experiment. This approach of combining comprehensive methods with the Euler or RANS flow equations is known as loose coupling (LC) or delta-load coupling (DC) [7].

Although a formal proof of solution-convergence to a time-periodic state has not yet been obtained for the LC/DC method, it has been applied when the flow is periodic in time as in forward flight at constant speed [7]. However, in general the LC/DC is not applicable when the flow is transient, for example, accelerating and decelerating rotors or maneuver [8]. In recent work some of the restrictions of the LC/DC methods have been partially alleviated by using a time-response method, starting from the final solution of the LC approach [9]. In order to model transient cases in a general and comprehensive manner, time-accurate (TA) methods in which the flow equations are directly coupled with the structural equations, are being developed. The use of time-accurate methods for simple blades with modal and finite-element structural models in conjunction with the Euler equations are demonstrated in Refs. 10 & 11.

The present research is a continuation of the earlier effort to develop an analysis capability using the Euler equations [10, 11]. Here, it is extended to the use of the RANS equations and validated with public domain data from the HART II (the Higher harmonic control Aeroacoustic Rotor Test II) wind tunnel test, a full rotorcraft configuration that includes deflection data [12]. The aeroelastic responses are computed by time accurately integrating the RANS equations and modal structural equations. Only independent windtunnel model parameters such as rotating speed, shaft angle, and control angles are used as input.

## 2. APPROACH

### 2.1 Domain-Based Approach

The structural system is physically much stiffer than the fluid system, and the numerical matrices associated with structures are orders-of-magnitude stiffer than those associated with fluids. In addition, structural systems have internal discontinuities such as skin-spar-rib of a blade whereas fluid systems have field discontinuities such as shockwaves. It is numerically inefficient to solve both systems using a single numerical scheme (see section on Sub-Structures in [13]). Therefore, a domain decomposition approach is used here where fluids and structures are solved in separate computational domains.

Guruswamy and Yang [14] presented a numerical integration method, based on the Arbitrary-Lagrange-Eulerian [15] approach, to solve this problem by independently simulating the flow using finite-differences to solve the transonic small-perturbation equation and finite-elements to model the structures. This method uses a finite element mesh with vertices that may be moved with the structure, and a finite-difference flow grid that also moves with rotor blades. Grid movements are matched at fluid/structure boundaries. The solutions were coupled only at the boundary interfaces between fluids and structures. The coupling of solutions at boundaries can be done either explicitly or implicitly. This domain-based approach allows one to take full advantage of state-of-the-art numerical procedures for individual disciplines. This coupling procedure was extended to three-dimensional problems and then incorporated into several advanced aeroelastic codes, such as XTRAN3S [16]. It was demonstrated that the method can also be extended to model fluids with the Euler/Navier-Stokes equations on moving grids [17, 18] for fixed-wing aircraft.

### 2.2 CFD Module

In this paper, the Reynolds-averaged Navier-Stokes equations [19] are numerically solved using the Pulliam-Chaussee diagonal form of the Beam-Warming central difference algorithm [20], along with the one-equation Spalart-Allmaras turbulence model [21] on an overset grid as implemented in the OVERFLOW code [22]. The unsteady pressures needed for aeroelastic computations are computed time accurately using the RANS equations. The code has a fluid/structure interfacing capability specific for forces and deformations defined along blade axis [23].

### 2.3 Aeroelastic Equations of Motion

The method of solution is based on the modal form of Lagrange's equations of motion. From modal analysis, the displacement vector  $\{d\}$  can be expressed as:

$$\{d\} = [\psi] \{q\} \quad (1)$$

where  $[\psi]$  is the 1-D modal matrix defined along blade axis and  $\{q\}$  is the generalized displacement vector. The final matrix form of the modal aeroelastic equations of motion is:

$$[M] \ddot{\{q\}} + [G] \dot{\{q\}} + [K] \{q\} = \{F\} \quad (2)$$

where  $[M]$ ,  $[G]$ , and  $[K]$  are the modal mass, damping, and stiffness matrices, respectively.  $\{F\}$  is the generalized aerodynamic force vector defined as

$$\{F\} = \frac{1}{2} \rho U^2 [\psi]^T \{L\} \quad (3)$$

where  $L$  is the vector of integrated sectional lift values of , moments and chord wise forces at control sections along the span,  $\rho$  is the free-stream density, and  $U$  is the local speed of the blade section. The structural damping  $G$  is assumed to be negligible compared to aerodynamic damping. The aerodynamic unsteady load vector  $\{L\}$  is computed by solving the RANS equations.

The aeroelastic equations of motion (2) are solved with a numerical integration scheme based on the linear-acceleration method [24] which is a member of the Newmark-family of direct integration algorithms. It assumes a linear variation in acceleration of the structure from time  $t$  to time  $t + \Delta t$ . The values of displacements, velocities and accelerations are known at time  $t$ , and the same values are unknown at time  $t + \Delta t$ . The linear acceleration assumption is adequate for the present computations, since the time-step size required for the fluids solver is an order of magnitude smaller than that required for the structural solver [4]. Assuming a linear variation of the acceleration, velocities and displacements at the end of a time interval  $t + \Delta t$  can be derived as follows:

$$\ddot{\{q\}}_{t+\Delta t} = [D] (\{F\}_{t+\Delta t} - [G] \{v\} - [K] \{w\}) \quad (4a)$$

$$\dot{\{q\}}_{t+\Delta t} = \dot{\{q\}}_t + \left(\frac{\Delta t}{2}\right) \ddot{\{q\}}_t + \left(\frac{\Delta t}{2}\right) \ddot{\{q\}}_{t+\Delta t} \quad (4b)$$

$$\{q\}_{t+\Delta t} = \{q\}_t + (\Delta t) \dot{\{q\}}_t + \left(\frac{\Delta t^2}{3}\right) \ddot{\{q\}}_t + \left(\frac{\Delta t^2}{6}\right) \ddot{\{q\}}_{t+\Delta t} \quad (4c)$$

where

$$[D] = \left( [M] + \left(\frac{\Delta t}{2}\right) [G] + \left(\frac{\Delta t^2}{6}\right) [K] \right)^{-1}$$

$$v = \dot{\{q\}}_t + \left(\frac{\Delta t}{2}\right) \ddot{\{q\}}_t$$

$$w = \{q\}_t + (\Delta t) \dot{\{q\}}_t + \left(\frac{\Delta t^2}{3}\right) \ddot{\{q\}}_t$$

These equations can also be derived using a second-order, time-accurate central-difference scheme, which falls into the explicit form of Newmark's time integration method [24]. The scheme described above is non-dissipative and does not lead to any nonphysical aeroelastic damping. To obtain physically accurate responses, it is necessary to use the same integration time-step for both the fluid and aeroelastic equations of motion. It is noted that the time-step size required to solve the RANS equations is an order of magnitude smaller than that required to solve the aeroelastic equations of motion (3). Therefore the time-step dictated by the RANS solver is also used to solve the aeroelastic equations.

The step-by-step integration procedure for obtaining the aeroelastic response is as follows: The grid for the flow solver is obtained using a dynamic grid generation method based on assumed initial values for the displacement  $\{q\}$ . Using this grid, the aerodynamic force vector  $\{F\}$  at time  $t + \Delta t$  is computed using the flow solver. Based on this aerodynamic vector, the new displacements at time  $t + \Delta t$  are

computed by solving Eq. 4c. This process is repeated at every step to advance the aerodynamic and structural equations of motion forward in time until the final response is obtained.

### 3. RESULTS FOR FULL ROTORCRAFT CONFIGURATION

In this paper public domain experimental data for HART II wind tunnel model [12] is used for validation. The test is a part of an international program comprising the German Aerospace Center (DLR), the German-Dutch Wind Tunnels (DNW) foundation, the French national aerospace laboratory National D'Etudes et de Recherches Aerospatiales (ONERA), NASA and the United States Army. The public domain HART II helicopter model that was tested in the wind-tunnel is shown in Figure 1. A unique feature of this test is that the data includes both measured aerodynamic forces and structural deformations.

The blades are 2 meters long, with 0.121m chord, and consist of NACA 23012 airfoil sections. Each blade has a built-in, -8 deg linear twist and a square tip.

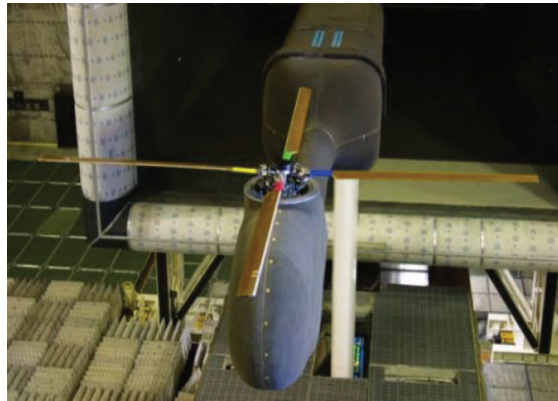


Figure 1. HART II wind tunnel model.

In this effort, the first flapping, torsion, and lead-lag modes taken from a shake test [12] are selected to model the structural properties. A structured grid [23] suitable for solving the RANS equations using the SA turbulence model consisting of 27 million points, in 32 near-body grid zones and 23 million points within 40 off-body grid zones is utilized. The surface grid and the grid near the tip are shown in Figs. 2 and 3, respectively. More details regarding the adequacy of this grid for the HART II configuration can be found in Ref. 23.

The base-line (BL) case, with an advance ratio  $\mu = 0.15$ , shaft angle of 4 deg, and blade rotational speed of 17 revolutions per second, was selected for the computations. At these conditions, the tip Mach number is 0.6387. The collective, lateral-cyclic, and longitudinal-cyclic pitch angle amplitudes taken from measurements are 3.20, -2.0, and 1.1 deg, respectively.

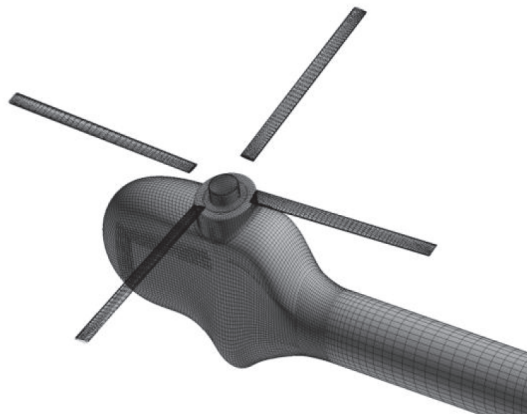


Figure 2. Surface grid for HART-II configuration (Ref. 23).

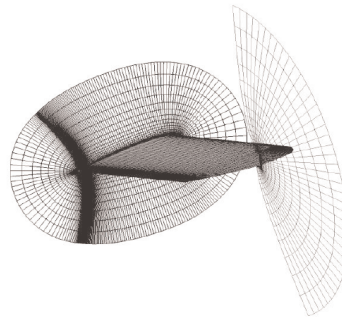


Figure 3. Grid details near the blade tip (Ref. 23).

In order to establish the adequacy of the time step, computations were performed for BL conditions on the isolated blade of the HART II system with varying time steps. The near-body grids for the blade, root, and tip have 1000000, 260000, and 150000 grid points, respectively. This grid is considered representative of the full rotor system since the same grid topology is repeated for all four blades. Computationally it is substantially less expensive to establish the time-step required to obtain time-accuracy by using the isolated blade.

The blade was rotated in integral multiples of 1200 steps per revolution (NSPR) starting at 1200. Figures 4 and 5 show plots of  $C_n$  and  $C_m$  with respect to azimuth, respectively.  $C_n$  converges around NSPR = 4800. The values for  $C_m$  are small since it is measured at the elastic axis very close to quarter chord, its convergence is slightly slower than that obtained for  $C_n$ . However the results are very close between NSPR = 6000 and 7200. All subsequent computations were performed with NSPR = 6000.

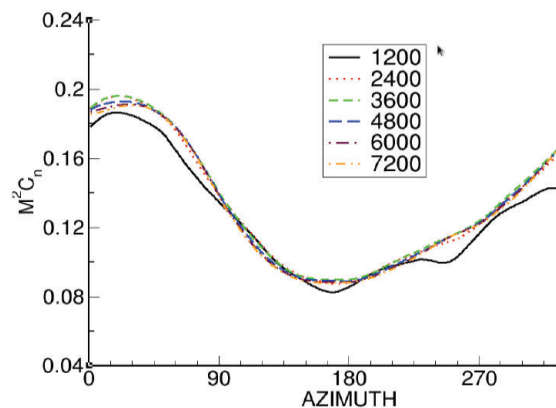


Figure 4. Effect of time step on  $C_n$  for baseline case.

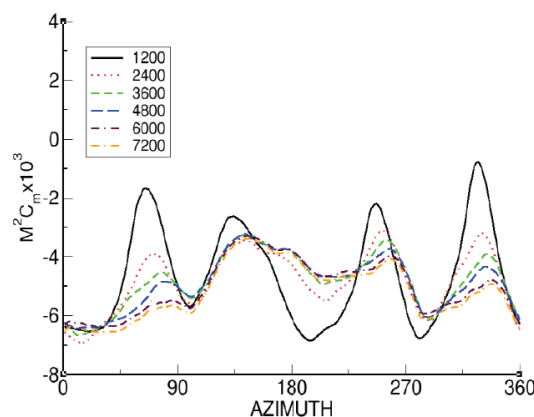


Figure 5. Effect of time step on  $C_m$  for baseline case.

Time accurate computations for the full rotorcraft configuration were found to require about five revolutions for the responses to converge. Figure 6 shows the response of the tip twist angle for 6 revolutions. Responses converge between the 4th and 5th revolutions. The results presented hereafter are from the 5th revolution.

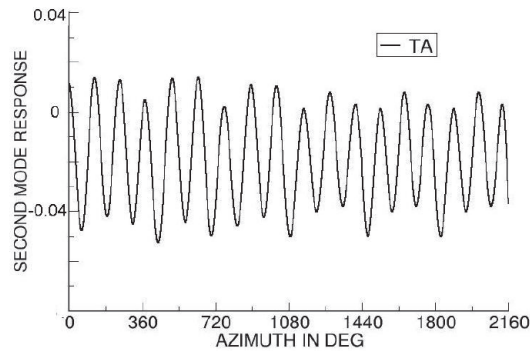


Figure 6. Second mode response for base line case.

Figure 7 shows a plot of the sum of the aeroelastic responses of the tip twist angle obtained using Eq. (1) and the rigid twist angle from prescribed control angles, both taken from the 5th revolution. Time accurate results compare well with experimental data until 270 deg azimuth. (Rigid motion of the blade is also shown for reference.) The experiment shows four extrema in response, whereas the TA computation shows five extrema. Between five and six extrema are expected since the blade oscillates in torsion approximately 2.7 times per revolution. Additional details regarding the experiment than currently published, such as uncertainties in measurements may help resolve the differences between computation and experiment.

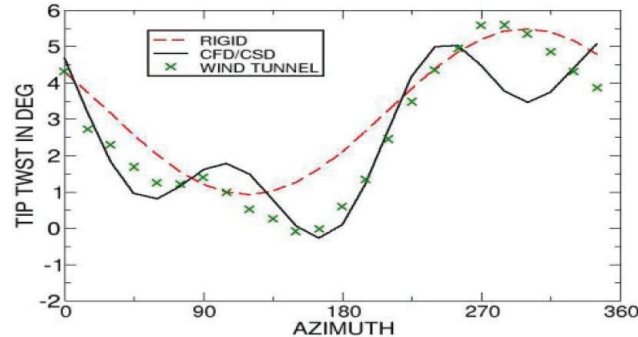


Figure 7. Comparison of tip twist angles at fifth revolution.

To date rotorcraft community tends to compare time-responses of forces between experiment and CFD/CSD computations. Start time of a force response in an experiment is either not available or has uncertainties. Often unprecedented procedures such as arbitrarily removing the mean from the computations is followed [7] in LC methods that results in better comparisons with experiments. On the other hand to minimize uncertainties fixed wing community historically has preferred [3, 24] to compare results in frequency domain by performing Fourier transformation [25]. In addition flutter computations needs unsteady airloads data in the form of Fourier coefficients [26]. In this paper Fourier coefficient are compared between experiment and CFD/CSD computations.

Fourier transformations were applied to the airloads to compute magnitudes and phase angles up to 20 harmonics with respect to the azimuth of the first blade. Figure 8 shows the comparison between the computed and flight sectional normal force magnitude at  $r/R = 0.87$ . The differences between the two data sets are slightly larger for the first four harmonics. The magnitudes become small after the 5th harmonic.

Figure 9 shows the scaled phase angle at various harmonics. The computed and measured phase



angles are scaled by the ratio of the magnitude of sectional normal force at a given harmonic to the magnitude of the sectional normal force at the first harmonic (obtained from Figure 8). The phase angles are scaled to eliminate the effects of noise at higher harmonics [25]. The computed scaled values compare reasonably well with the scaled values of experimental data.

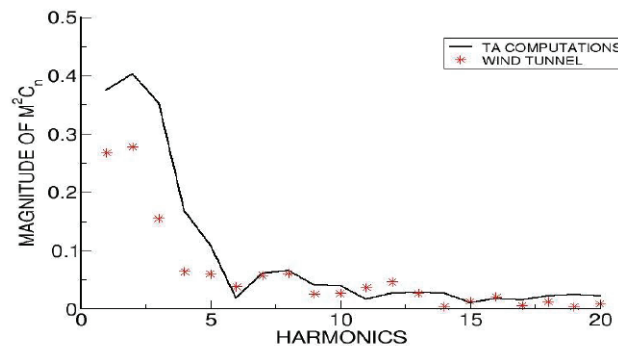


Figure 8 Sectional normal force at 87% radial station of HART II configuration for baseline case.

Figure 10 shows the comparison between computed and flight pitching-moment magnitude at  $r/R = 0.87$ . The comparison is similar to that observed for sectional normal force. Figure 11 show the scaled phase angle for the pitching moment. As in Figure 9 the computed results agree reasonably well with the experimental data.

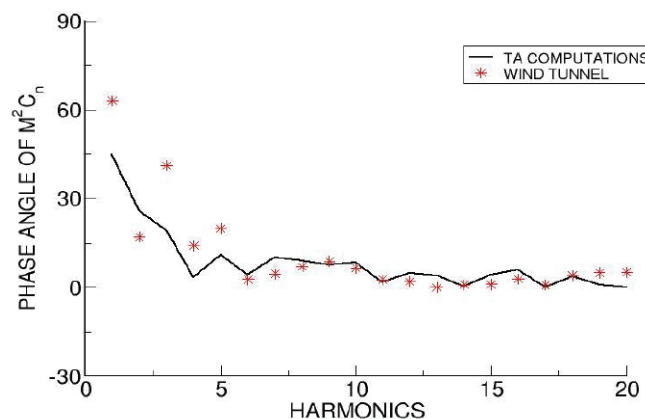


Figure 9 Phase angles of sectional normal force at 87% station radial station of HART II configuration for base line case.

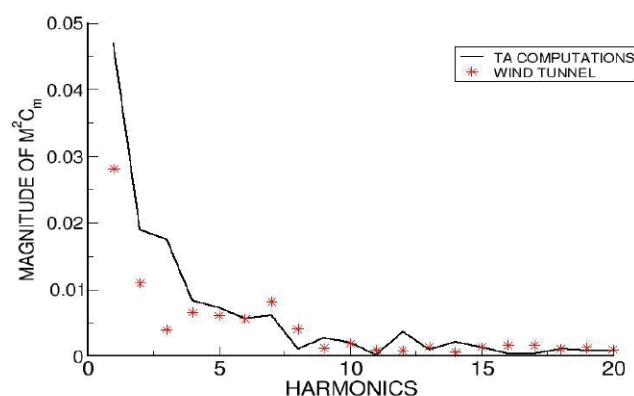


Figure 10 Pitching moment at 87% radial station of HART II configuration for base line case.

The differences between the computed and measured data seen in Figs. 7 to 11 can be attributed to the complexity of the HART II model compared to the simple blade for which better comparisons are obtained in Ref. 10. The presence of the body may have resulted in the associated hub modes influencing the experimental data. In this paper only the first flapping, torsion and lead-lag modes available in the public domain at the time this research were used. Additional modes may be required to reduce the observed differences between computational and experimental data. To date all computations made for HART II by other researchers have included only blade structural properties.

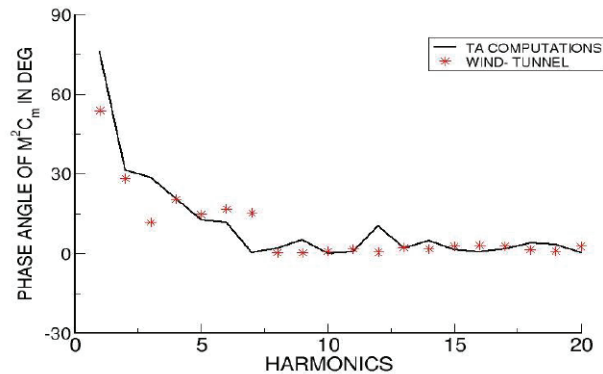


Figure 11 Phase angles of pitching moment at 87% section radial station of HART II configuration for baseline case.

Figure 12 shows a snapshot of vorticity magnitude and, surface pressure on the HART II body. Wakes are modeled in the LC/DC approach [7], whereas here they are directly computed using the RANS equations. The development of tip-vortices and bladewake structure can be seen in Figure 12. This predictive capability of RANS approach used in the used in present time-accurate simulation helps understanding complex flow phenomena such as blade-vortex interactions, dynamic stall etc. and their impact on structural responses.

All computations were performed on the Pleiades super cluster of NASA [27]. One revolution for the full HART II configuration required about 5 hours of wall clock time using 1024 processors.

#### 4. CONCLUSIONS

Fluid/structure responses are computed for rotating blades by time-accurately integrating the Navier-Stokes flow equations together with the modal structural equations. It is shown that such computations can be performed with only primitive inputs from the measurements. Wakes are computed using the Navier-Stokes equations, rather than using a linear aerodynamics model as in comprehensive analyses. Application of time-accurate coupling resulted in a reasonable comparison with wind tunnel data. Computations using measured modal data compare better with experiment than obtained using a beam finite element model for the HART II configuration. This investigation advances the state-of-the-art in modeling and analysis of complex rotorcraft configurations, and demonstrates a procedure to compute transient flight conditions.

#### 5. ACKNOWLEDGEMENTS

The author sincerely thanks Doug Boyd of NASA Langley Research Center for providing the grid for the flow solver and consultations in implementing aeroelastic motion in overset grid topology. Consultations with Pieter Buning of NASA Langley Research Center and Dennis Jespersen of NASA Ames Research center regarding overset methods and parallel computing were very valuable. Help from Tim Sandstrom of NASA Ames Research Center in flow animation aided in a better understanding of the flow characteristics. This work was performed under Subsonic Rotary Wing and High End Computing projects of NASA.

#### REFERENCES

- [1] Bielava, R. L., "Unsteady Aerodynamics and Flutter," *Rotary Wing Structural Dynamics and Aeroelasticity*, AIAA Education Series, Washington D.C., 1992, pp. 379-454.



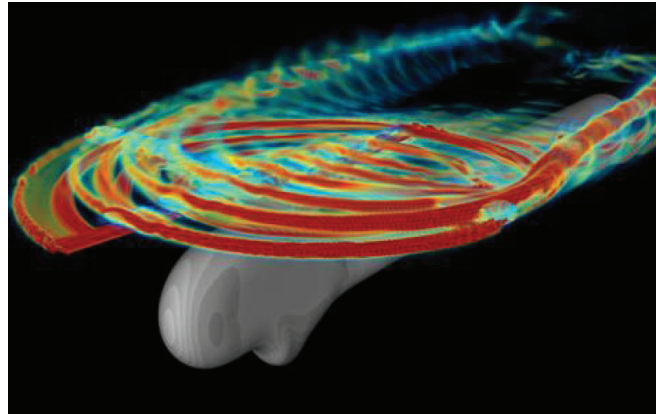


Figure 12 Snapshot of body surface pressures (black & white) and vorticity magnitude (color) for base line case of HART II configuration.

- [2] Narramore, L., "Computational Fluid Dynamics Development and Validation for Helicopter," *AGARD CP-552*, August 1995.
- [3] Guruswamy, G. P., "Unsteady Aerodynamic and Aeroelastic Calculations for Wings Using Euler Equations," *AIAA J.*, Vol. 28, No. 3, March 1990, pp. 461-469.
- [4] Guruswamy, G. P., "Aeroelastic Stability and Time Response Analysis of Conventional and Supercritical Airfoils in Transonic Flow by the Time Integration Method," Ph. D. Thesis, Purdue University, December 1980.
- [5] Datta, A., and Chopra, I., "Validation and Understanding of UH-60A Vibratory Loads in Steady Level Flight," *J. of the American Helicopter Society*, Vol. 49, No 3, July 2004, pp. 271-287.
- [6] Tanabe, Y. and Saito, S., "A CFD/CSD Loose Coupling Approach for Rotorcraft Blade Deformation," *Japan Aerospace and Exploration Agency*, JAXA-RR-08- 008E, March 2009.
- [7] Jung, S. M., You, Y. H., Kim, J. W., Sa, J. H., Park, J. S. and Park, S. H., "Correlation of Aeroelastic Response and Structural Loads for a Rotor in Descent," *J. of Aircraft*, Vol. 49, No. 2, March-April 2012, pp. 398-406.
- [8] Kunz, D. L., "Comprehensive Rotorcraft Analysis: Past, Present and Future," *AIAA 2005-2244*, April 2005.
- [9] Abhishek, A. and Chopra, I. "Prediction and Validation of UTTAS Pull-up Maneuver Using CFD/CSD Coupling," *AIAA-2011-1774*, April, 2011.
- [10] Guruswamy, G.P., "A Modular Approach to Euler Equations Based Aeroelasticity of Helicopter Rotor Blades," *AIAA-2008-2179*, April 2008.
- [11] Guruswamy, G.P., "Computational-Fluid-Dynamics and Computational- Structural-Dynamics Based Time-Accurate Aeroelasticity of Helicopter Blades," *J. of Aircraft*, Vol. 47, No. 3, May-June 2010, pp. 858-863.
- [12] Van der Walla B. G, Burleyb, C. L., Yuc, Y., Richard, H., Pengele, K. and Beaumierf, P., "The HART II Test—measurement of Helicopter Rotor Wakes," *Aerospace Science and Technology*, Vol. 8, Issue 4, June 2004, pp. 273-284.
- [13] Zienkiewicz, O. C. Taylor, R. L., and Zhu, J. Z., "*Substructures*," *The Finite Element Method Its Basis and Fundamentals*. 3rd edition, McGraw Hill Book Company (UK) Limited, Maidenhead, Berkshire, England, 1977, pp. 132-134.
- [14] Guruswamy, P. and Yang, T.Y., "Aeroelastic Time Response of Thin Airfoils by Transonic Code LTRAN2," *International J of Computers and Fluids*, Vol. 9, No. 4, 1981, pp. 409-425.
- [15] Hirt, C. W., Amsden, A. A., and Cook J. L., "An arbitrary Lagrangian-Eulerian computing method for all flow speeds," *J of Computational Physics*, Vol. 14, Issue 3, March 1974, pp. 227-253.
- [16] Borland, C. J. and Rizzetta, D., "XTRAN3S-Transonic Steady and Unsteady Aerodynamics for Aeroelastic Applications, Vol. I—Theoretical Manual," *AFWAL-TR-80-3107*, Dec. 1985.

- [17] Guruswamy, G. P., "ENSAERO—A Multidisciplinary Program for Fluid/ Structural Interaction Studies of Aerospace Vehicles," *Computing Systems Engineering*, Vol. 1, Nos. 2-4, 1990, pp. 237-256.
- [18] Guruswamy, G.P. "HiMAP - A Portable Super Modular Multilevel Parallel Multidisciplinary Process for Large Scale Analysis," *Advances in Engineering Software*, Elsevier, Vol. 31, Issue 8-9, Aug-Sept. 2000, pp. 617-620.
- [19] Peyret, R and Viviand, H, "Computation of Viscous Compressible Flows based on Navier-Stokes Equations," *AGARD-AG-212*, 1975.
- [20] Pulliam, T. H. and Chaussee, D. S. "A diagonal form of an implicit approximate factorization algorithm," *J of Computational Physics*, Vol. 39, No. 2, 1981, pp. 347-363.
- [21] Spalart, P. R, "Direct simulation of a turbulent boundary layer," *Jl of Fluid Mechanics*, Cambridge University Press (1988), 187, pp. 61-98.
- [22] Nichols, R. H., Tramel R. W., and Buning P. G., "Solver and Turbulence Model Upgrades to OVERFLOW 2 for Unsteady and High-Speed Applications," AIAA- 2006-2824, *AIAA 36th Fluid Dynamics Conference*, San Francisco, CA, June 2006.
- [23] Boyd, D. D., "HART-II Acoustic Predictions using a Coupled CFD/CSD method," *American Helicopter Society 65th Annual Forum*, May 2009, Grapevine, Texas.
- [24] Schuster, D. M., Heeg, J., Wieseman C. and Chwalowski, P. "Analysis of Test Case Computations and Experiments for the Aeroelastic Prediction Workshop," *AIAA Paper 2013-0788*, 51st AIAA Aerospace Sciences Meeting, Jan. 2013, Grapevine, Texas.
- [25] Guruswamy G. P., "CFD based Computations of Flexible Helicopter Blades for Stability Analysis," AIAA-2011-1875, AIAA/AHS Structural Dynamics Conf, Denver CO, April 2011.
- [26] Guruswamy, G. P., "Large Scale Aeroelastic Data for Design of Rotating Blades using Navier-Stokes Equations," AIAA-2012-5715., AIAA <sup>14th Multidisciplinary Conf.</sup>, Indianapolis, IN, Sept. 2012.
- [27] Guruswamy, G.P., "Large-Scale Computations for Stability Analysis of Launch Vehicles Using Cluster Computers," *J of Spacecraft and Rockets*, Vol. 48, no 4, July-August 2011, pp 584-588.